

ON THE TEMPORAL BEHAVIOR OF KARST AQUIFERS, ZAGROS REGION, IRAN: A GEOSTATISTICAL APPROACH

ZARGHAM MOHAMMADI¹ AND MALCOLM FIELD²

Abstract: A geostatistical approach was used to study temporal structures in a time series of discharge and electrical conductivity (EC) in 15 karst springs from the Zagros mountain range, Iran. Two types of temporal behaviors, a periodic structure and nugget effect, plus one or two temporal structures, were identified and interpreted. These correspond to characteristics of karst systems, such as the catchment area, percent of conduit flow, and general degree of karst development. Springs were grouped into three categories based on their ranges (e.g., residence time) obtained by variogram analysis. The first group of springs include those that present the same temporal behaviour in variograms of discharge and EC. These springs are characterized by generally constant EC with increasing discharge suggesting the existence of a large underground reservoir. The second group of springs are those with varying temporal periodic behavior in variograms of discharge and EC. Positive correlation between discharge and EC values is the main characteristic of these springs and is interpreted to result from a piston-flow system in poorly developed karst aquifers. The third group of springs includes those that exhibit different temporal behaviors when compared with the periodic and non-periodic variograms. This group exhibits a negative correlation in scatterplots of discharge versus EC values suggesting a well-developed solution-conduit system that facilitates rapid response of the karst system to precipitation events. This study's results document the role of variogram analysis in delineating temporal structures of spring behaviors by means of time series of discharge and EC. Variogram analysis can be considered as a valuable tool for hydrogeological investigations in karstic terranes.

DOI: 10.4311/jcks2009es0079

INTRODUCTION

Karst groundwater is a major water resource in many regions of some countries such as China, Turkey, Iran, the United States, etc. Karstic-carbonate formations cover about 11% of the land area in Iran (185,000 km²) and 55% of the Zagros Region (Raeisi, 2004). Carbonate rocks become karstic aquifers by dissolution processes, typically referred to as karstification. Karstification creates a significant heterogeneity of the permeability within the aquifer. Karst development processes and several methods intended to characterize karst systems have been extensively presented in Palmer (2007), Ford and Williams (2007), Bakalowicz (2005), White (1988), Gillieson (1996), Mangin (1994), and Milanović (1981).

The hydrogeological study of karst aquifers is particularly difficult because of the complex and heterogeneous character of the karstic massif and the limited number of available wells that permit hydrogeological observation (Padilla and Pulido-Bosch, 1995; Panagopoulos and Lambrakis, 2006; Mohammadi and Raeisi, 2007). As a result, studies on the function and hydrodynamic behaviour of karst aquifers are focused on the analysis of the characteristics of karst springs. Two commonly measured parameters are discharge and electrical conductivity (EC) that are often presented as a time series. These parameters are widely used by karst researchers because these parameters provide

reliable results regarding karst-aquifer characteristics and are relatively easy and inexpensive to collect, especially in less developed area such as the Zagros Region in Iran. Time-series variations of physico-chemical parameters of springs have been used by many authors for assessing hydrogeochemical aspects of karst aquifers (e.g., Hess and White, 1988; Scanlon and Thraikill, 1987; Raeisi and Karami, 1997; Lopez-Chicano et al., 2001; Desmarais and Rojstaczer, 2002; Karimi et al., 2005a; and Mohammadi et al., 2007). Generally, these authors focused on temporal variations of discharge and chemical parameters caused by a heavy precipitation event in terms of internal and external factors involving the karst system studied. Many authors (e.g., Mangin, 1984; Moore, 1992; Padilla and Pulido-Bosch, 1995; Larocque et al., 1998; Kovacs et al., 2005; and Manga, 1999) applied correlation and spectral analysis on the time series of springs to extract further information about time lag, periodicity, and residence time.

Variogram analyses are extensively used in hydrology (e.g., Bacchi and Kottegoda, 1995; Holawe and Dutter,

Disclaimer: The views expressed in this paper are solely those of the authors and do not necessarily reflect the views or policies of the U.S. Environmental Protection Agency.

¹Department of Earth Science, Shiraz University, Shiraz, Iran, z mohamad@shirazu.ac.ir

²U.S. Environmental Protection Agency, National Center for Environmental Assessment (8623P), 1200 Pennsylvania, Ave., NW, Washington, DC 20460, USA, field.malcolm@epa.gov

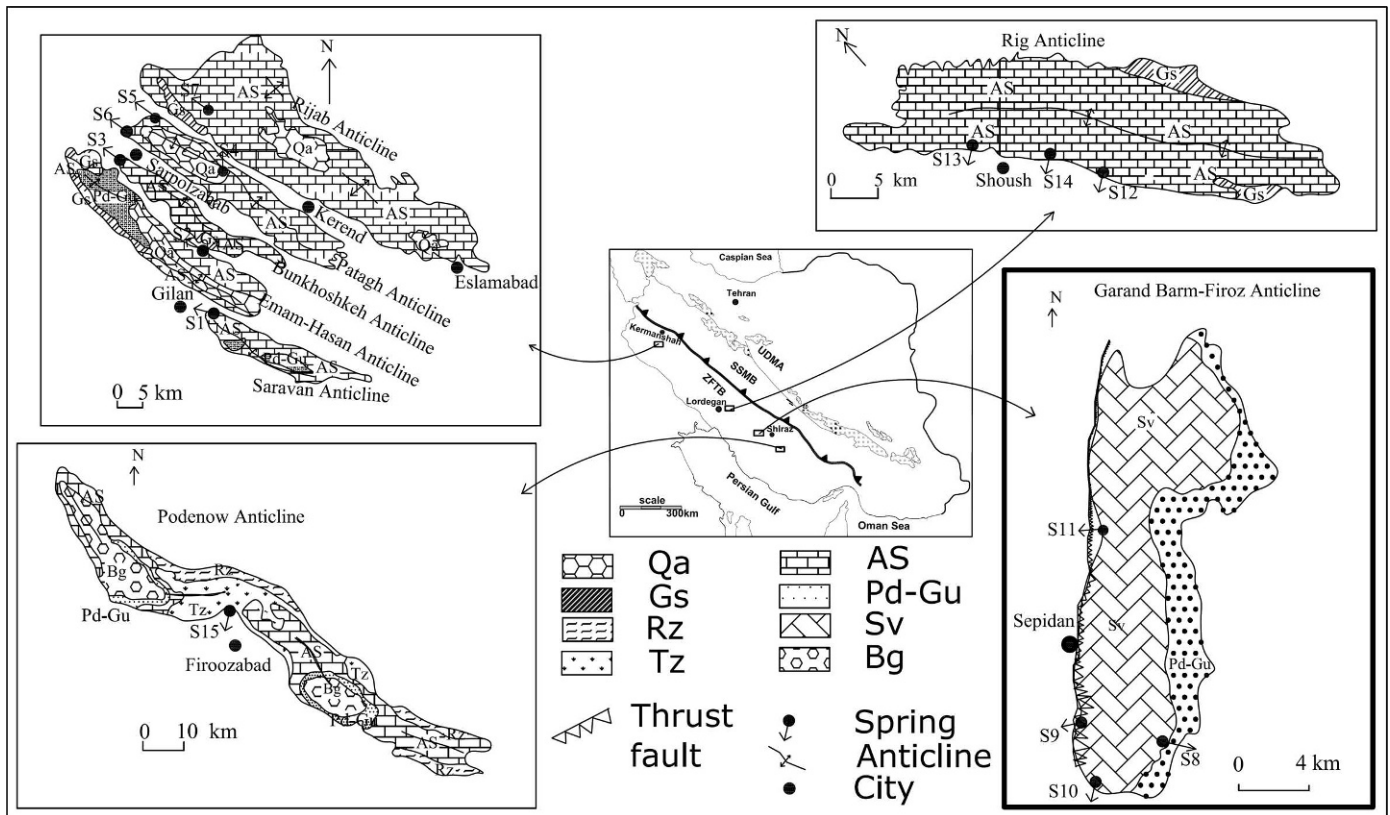


Figure 1. Simplified geological map of the selected aquifers in the Zagros mountain range. See Table 1 for a description of map symbols of depicted geological units.

1999; Berne et al., 2004; Kyriakidis et al., 2004; and Buytaert et al., 2006), but its contribution to a time series of physico-chemical parameters of springs is rare (e.g., Rouhani and Wackernagel, 1990; Goovaerts et al., 1993; Kolovos et al., 2004; and Silliman et al., 2007). Rouhani and Wackernagel (1990) applied variogram analysis to monthly piezometric data at 16 observation wells in a basin south of Paris, France. Two temporal structures were determined by the variogram analysis, including the 12-month seasonal and the 12-year climatic cycles. Multivariate geostatistical analysis was applied to spring-water-solute contents measured in 86 springs situated in Belgium by Goovaerts et al. (1993).

In this study, we use variogram analyses to evaluate the time-series data of discharge and EC measurements obtained from 15 springs located in the Zagros Region of southern Iran (Fig. 1). The study is aimed at improving our understanding of the temporal dynamics of the karst system in the area. The objectives of this study, with the expectation that a better understanding of karstic aquifers may be obtained, are (1) determination of the temporal structures in the time series of discharge and EC, (2) exploration of new information on the characteristics of the karst systems, and (3) evaluation of the potential of variogram analysis for studying karst development.

GEOLOGICAL AND HYDROGEOLOGICAL SETTINGS

The Zagros Region is located in south-west Iran. The climate is semi-arid in the uplands and arid in the lowlands (south of Iran). Precipitation exhibits large spatial and temporal variability with a mean annual precipitation in the Zagros region of about 450 mm, with a range of 150 to 750 mm. Runoff is an aggregation of several hydrological river basins that discharge to the Persian Gulf. The high elevation areas of the Zagros Region are the zones where the rivers originate; the main rivers flowing in the Zagros region are Karoun River, Dae River, Karkhe River, Hele River, Mond River and Zohre River. Karoun River is the Zagros' most important river with the highest amount of flow and many tributaries in upstream sub-watersheds, the largest of which is the Dez River. Karoun River is a major source of water for 4.5 million inhabitants in the south of Iran (KWPA, 2009).

Iran is geologically a part of the Alpine-Himalayan orogenic belt. The Zagros mountain range extends from the northwest to southeast of Iran and consists of three NW-SE trending parallel zones (Fig. 1): (1) the Urumieh-Dokhtar Magmatic Assemblage (UDMA); (2) the Sanandaj-Sirjan Metamorphic Belt (SSMB); and (3) the Zagros Fold and Thrust Belt (ZFTB). The ZFTB is the study area of this paper.

Table 1. Stratigraphic column of geological units depicted in Figure 1.

Symbol on Figure 1	Geologic Unit	Geologic Age	Composition
Qa	Recent alluvium
Gs	Gachsaran Formation	Miocene	Gypsum, marl and salt
Rz	Razak Formation	Lower Miocene	Silty marl to silty limestone with interbedded layers of gypsum
Tz	Transition zone	Lower Miocene	Transition between Asmari and Razak Formations
As	Asmari Formation	Oligocene-Miocene	Limestone, dolomite
Pd-Gu	Pabdeh-Gurpi Formation	Paleocene-Oligocene	Marl, shale and marly limestone
Sv	Sarvak Formation	Upper Paleocene	Limestone
Bg	Bangestan Group	lower Paleocene	Limestone, shale, marl

The stratigraphy and structural framework of the ZFTB were studied in detail by James and Wynd (1965), Stocklin and Setudehnia (1977) and Alavi (2004, 2007). The ZFTB is about 12-km thick and consists mainly of limestone, marl, gypsum, sandstone and conglomerate. Since the Miocene age, it has been folded into a series of huge anticlines and synclines. Most of the carbonate rock outcrops are of Cretaceous and Tertiary age. The most important karst features in the ZFTB are karren, grikes, and springs, and to a lesser extent, caves and sinkholes. Most of the springs are permanent with a high percentage of spring discharge from base flow. The ZFTB is characterized by a repetition of long and regular anticlinal and synclinal folds. The anticlines normally form mountain ridges of limestone and the synclines normally form valleys and plains. Most of the karst formations in the ZFTB are sandwiched between two impermeable formations that form broad highland independent aquifers (Raeisi, 2004; Raeisi and Laumanns, 2003). Several anticlines from different parts of the ZFTB were selected for this study. Simplified geological maps of these anticlines are presented in Figure 1 and a description of the geological units in Table 1.

SEVERAL ANTICLINES IN THE ALVAND RIVER BASIN

The Alvand river basin comprises seven main anticlines (Karimi, 2003), five of which are considered in this study, and include the Saravan, Emam-Hasan, Bunkhoshkeh, Patagh, and Rijab anticlines (Fig. 1). These anticlines are located ~150 km west of the Kermanshah located in the south-western part of Iran (Fig. 1), follow a northwest-southeast trend, and are mainly composed of the Asmari limestone. The geologic formations in this area are, from youngest to oldest: 1) recent alluvium; 2) Gachsaran gypsum and marl; 3) Asmari dolomite and limestone; and 4) Pabdeh-Gurpi marl and shale with interbedded, thin marly limestone (Fig. 1). The core of the anticlines is composed of the Asmari formation and is situated between the impermeable upper Gachsaran and lower Pabdeh-Gurpi formations (Karimi et al., 2005b). The dense and thick bedded Asmari limestone in the anticlines has

numerous joints and fractures with limited solution features and small shelter caves (Karimi et al. 2005b). Generally, the southern flanks are hydraulically disconnected in most parts of the anticlines (Karimi, 2003), except in the plunge areas. Groundwater from the above aquifers discharge from seven main springs including Gilan (S1), Golin (S2), Sarabgarm (S3), Marab (S4), Piran (S5), Gharabolagh (S6) and Rijab (S7) Springs (Fig. 1 and Table 2). There is no hydraulic connection between these springs except the Marab (S4), Piran (S5) and Gharabolagh (S6) which emerge from Patagh Anticline. However, the catchment areas of the springs were mapped without any overlap in their areas (Karimi, 2003).

THE BARM-FIROOZ AND GAR ANTICLINES

The Barm-Firooz and Gar Anticlines are located 80 km northwest of Shiraz on a general northwest trend of the Zagros mountain range. The cores of the anticlines are comprised of the calcareous Sarvak formation, which is overlain by impermeable Pabdeh-Gurpi formations (Fig. 1). The most important tectonic feature in this area is a northwest trending thrust fault (Fig. 1). Groundwater from the Sarvak aquifer discharges mainly from Sheshpir (S8), Berghan (S9), Morikosh (S10), and Tangkelagari (S11) Springs (Fig. 1). The most important karst features in the catchment area of Sheshpir Spring (S8) is the presence of 255 sinkholes (Raeisi and Karami, 1997). Several normal faults and one thrust fault have resulted in an extensive brecciated zone in the catchment area of Berghan Spring (S9). No sinkholes or caves are present in the catchment area of Berghan Spring (S9). It seems that karst is developed as a network of interconnected small fissures and pores (Raeisi and Karami, 1997) and with minimal karstification. No hydraulic connection between the catchment area of Sheshpir spring (S8) and three other springs has been reported.

THE RIG ANTICLINE

The Rig anticline is located in Southern Iran near the city of Lordegan. The main formations in this area are the Gachsaran (Miocene), Asmari (Oligocene-Miocene), and

Table 2. Data sets characteristics used in the analysis.

Spring Name	Code on Figure 1	Anticline	Sampling Interval	Sampling Period	Data Reference
Gilan	S1	Saravan	Weekly ^a	09/00–09/01	Karimi (2003)
Golin	S2	Emam-Hasan	Weekly ^a	09/00–09/01	Karimi (2003)
Sarabgarm	S3	Bunkhoshkeh	Weekly ^a	09/00–09/01	Karimi (2003)
Marab	S4	Patagh	Weekly ^a	09/00–09/01	Karimi (2003)
Piran	S5	Patagh	Weekly ^a	09/00–09/01	Karimi (2003)
Gharabolagh	S6	Patagh	Weekly ^a	09/00–09/01	Karimi (2003)
Rijab	S7	Rijab	Weekly ^a	09/00–09/01	Karimi (2003)
Sheshpir	S8	Gar and Barm-Firoz	Daily ^b	03/90–11/91	Karami (1993); Pezeshkpoor (1991)
Berghan	S9	Gar and Barm-Firoz	20 days	03/90–11/91	Karami (1993); Pezeshkpoor (1991)
Morikosh	S10	Gar and Barm-Firoz	20 days	03/90–11/91	Karami (1993); Pezeshkpoor (1991)
Tangelagari	S11	Gar and Barm-Firoz	20 days	03/90–11/91	Karami (1993); Pezeshkpoor (1991)
Atashgah	S12	Rig	Weekly ^a	05/02–09/03	Keshavarz (2003)
Shosh	S13	Rig	Weekly ^a	05/02–09/03	Keshavarz (2003)
Enakak	S14	Rig	Weekly ^a	05/02–09/03	Keshavarz (2003)
Ghomp	S15	Podenow	Daily ^b	04/96–09/97	Karimi (1998)

^a One week during rainy season and one or two weeks during dry season.

^b Daily during rainy season and two weeks during dry season.

Pbdeh-Gurpi (Paleocene-Oligocene) Formations (Fig. 1). Rig Anticline is a box fold that mainly consists of the karstic Asmari Formation (Keshavarz, 2003). Numerous joint sets are observed in the Asmari Formation. There appears to be no concentrated recharge points, such as sinkholes or sinking streams, in this aquifer. The Atashgah Spring (S12), having a mean discharge rate of about 900 L s⁻¹, is the largest spring originating from the Rig Anticline (Fig. 1). Two other large springs, Shosh (S13) and Enakak (S14) Springs, emerge from the Rig anticline (Fig. 1).

THE PODENOW ANTICLINE

The Podenow anticline is located south of Shiraz, Iran. The geological formations in decreasing order of age consist of the Bangestan group (lower Palaeocene), Pabdeh-Gurpi (Palaeocene-Oligocene), Asmari (Oligocene-Miocene), Transition zone and Razak (Lower Miocene), as shown in Figure 1. The core of the Podenow anticline is composed of the limestone Asmari Formation which is sandwiched between the two impermeable Pabdeh-Gurpi (marl, shale and marly limestone) and Razak (silty marl to silty limestone with interbedded layers of gypsum) Formations (Fig. 1). This anticline is divided into eastern, central, and western parts based on the orientations of the anticline. The eastern and western sections follow the general northwestern trend of the Zagros mountain range (Karimi et al., 2005a). The largest spring on the southern flank is Ghomp Spring (S15 in Fig. 1).

MATERIALS AND METHODS

DATA COLLECTION

Electrical conductivity and discharge measurements from the 15 springs from the Zagros mountain range were used for this study. Sampling intervals and sampling periods for each spring are presented in Table 2. Electrical conductivity was measured by a portable ELE EC-meter in the field immediately after sampling. Spring discharge was measured by current-meter or triangular weir related to spring discharge and field conditions. Hydrogeological characteristics of the studied springs are presented in Table 3.

DATA ANALYSIS

Exploratory data analysis and variogram analysis were used for database analyses. Use of multiple data analyses techniques provides greater insight into the information contained in a database (Farnham et al., 2000; Silliman et al., 2007).

Exploratory-Data Analysis

Exploratory data analysis is a purely descriptive part of the study that allows for a good preliminary assessment of the collected data (Isaaks and Srivastava, 1989). There is no single statistical tool as powerful as a plot of the data (Chambers et al., 1983). The distribution of continuous variables can be depicted by a histogram with the range of data values discretized into a specific number of classes of equal width and the relative proportion of data within each

Table 3. Hydrogeological characteristics of the studied springs.

Spring Name	Elevation (m)	Watershed Area (km ²)	Annual Precipitation (mm)	Percent of Conduit Flow	Ratio of Recession Coeff. (a_1/a_2)	Ratio of Max. to Min. Discharges (Q_{\max}/Q_{\min})
Gilan	1413	110	473	8	0.57	1.58
Golin	1526	68.8	492	3.7	1	1.12
Sarabgarm	1191	204.1	454	5.4	75	1.35
Marab	1879	42	515	35	26.7	5.25
Piran	1176	26.7	460	15	1	1.39
Gharabolagh	1576	56.8	515	6.9	4.5	1.36
Rijab	1874	221	552	35	3.08	7.58
Sheshpir	2335	81	1334	24	11.5	4.56
Berghan	2145	19	798	23.7	2	3.92
Morikosh	2450	4.3	1122	31	2.7	15.5
Tangkelagari	2120	4.47	985	28	2.5	15.2
Atashgah	1710	62	930	13.5	4.4	1.91
Shosh	1500	18.2	910	21	2	5.69
Enakak	1750	5	890	25	2.2	7.6
Ghomp	1350	114.2	400.7	29.5	4.4	3.03

class (e.g., frequency) by the height of bars (Goovaerts, 1997). Important features of a distribution are its central tendency and measure of its spread and symmetry. The relationship between pairs of variables can be depicted in a scatterplot, which is the simplest and probably most informative method for comparing data pairs (Deutsch and Journel, 1992). The correlation coefficient is mostly used as a measure of bivariate relationships. Here, exploratory data analyses include histograms and probability plots of the discharge and EC data series for each spring and relationships among pairs of discharge and EC data as scatterplots. The data plots were developed using Statistica Software, Release 6 (StatSoft, 2001).

Variogram Analysis

The variogram approach is extensively used in geological and environmental sciences to assess the characteristics of spatially or temporarily distributed data (e.g., Isaaks and Srivastava, 1989; Goovaerts, 1997; Webster and Oliver, 2001). The variogram measures the spatial and/or temporal behavior of a variable of interest (Deutsch and Journel, 1992). It is easy to interpret the time axis as the location coordinate in the variogram analysis (Holawe and Dutter, 1999). Many papers in various disciplines have been published using variogram methods for different regionalized variables at different time scales of interest (e.g., Holawe and Dutter, 1999; Berne et al., 2004; Buytaert et al., 2006). Variogram modeling and analysis was accomplished using the program, VESPAR (Minasny et al., 2005).

Assuming the studied time series of observations is a realization of a random function Z , so that $z(t)$, $t = 1, 2, 3, \dots, m$, where $z(t)$ refers to observed values of discharge

or EC at time t and m is the length of sampling period. Given two times, t and $t + h$ inside the period of temporal attribute $z(t)$, the experimental variogram is a measure of one half the mean square error produced by assigning the value $z(t + h)$ to the value $z(t)$, as follow:

$$\gamma(h) = \frac{1}{2N(h)} \sum_{i=1}^{N(h)} [z(t+h) - z(t)]^2 \quad (1)$$

where $N(h)$ is the number of pairs of observations for a time separation, h . The shape of semivariograms is quantified by the behavior of the variogram at the origin (nugget effect), range, and sill.

The nugget effect is a measure of the variability of a variable within small time lengths. Normally the nugget effect is seen as a consequence of the limited number of observations with arbitrarily small time periods (Holawe and Dutter, 1999). Smaller nugget values translate into higher values of influence of small time lags. Therefore, nugget values can be interpreted as altering variables that can play a special role in a simulation model (Holawe and Dutter, 1999). The range, in the case of time dependence, is a measure related to the length of influence of a variable (Holawe and Dutter, 1999). The sill is a value of the covariance that becomes zero when the variogram reaches a constant value. This total sill is equal to the basic variance of the variable. Therefore, the sill is an indicator for the variance in the data field and, in the case of a time series, a measure of the temporal variability.

In order to describe the variogram structure, it is necessary to fit a model to the experimental variogram. The permissible models are presented by Isaaks and Srivastava (1989). The goodness of fit of different models can be

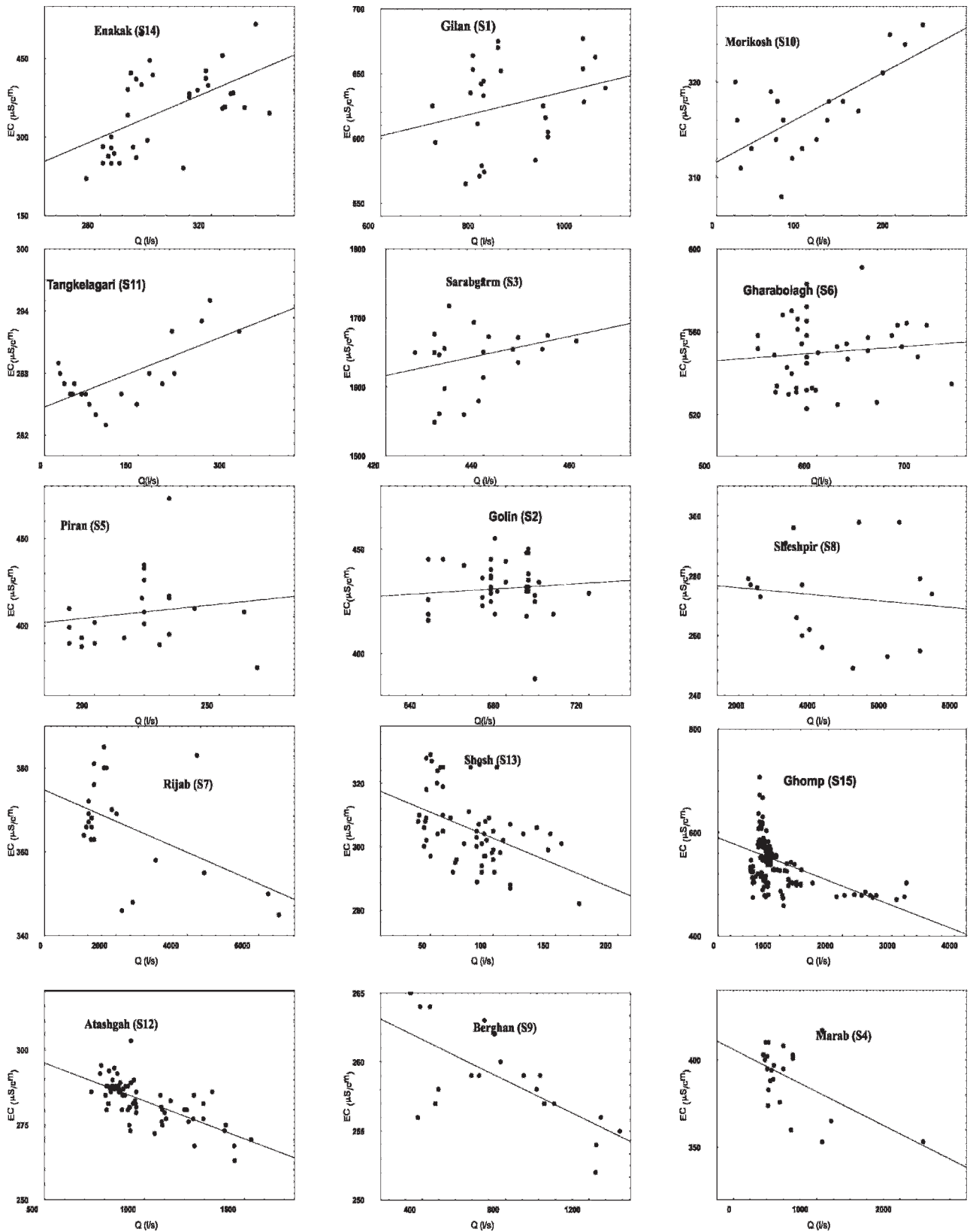


Figure 2. Scatterplots of discharge and EC values for springs.

Table 4. Descriptive statistics of discharge and electrical conductivity for studied springs.

Spring	Number of Samples	Mean	Median	Minimum	Maximum	Range	Std. Dev.	Skewness	C.V %
Gilan									
Discharge (L s ⁻¹)	40	861.1	820.5	704	1050	346	99.9	0.5	11.6
Elec. Cond. (μ cm ⁻¹)	40	626.2	630.5	565	677	112	33.8	-0.3	5.4
Golin									
Discharge (L s ⁻¹)	42	675.4	674	643	720	77	19.1	-0.3	2.8
Elec. Cond. (μ cm ⁻¹)	42	431.0	430.5	388	455	67	12.2	-0.8	2.8
Sarabgarm									
Discharge (L s ⁻¹)	41	438.8	438.5	426	459	33	8.8	0.7	2.0
Elec. Cond. (μ cm ⁻¹)	41	1644.8	1653	1549	1755	206	51.0	-0.2	3.1
Marab									
Discharge (L s ⁻¹)	42	646.9	481	354	2276	1922	427.1	2.8	66.0
Elec. Cond. (μ cm ⁻¹)	42	390.4	395	353	417	64	18.6	-0.8	4.8
Piran									
Discharge (L s ⁻¹)	40	218.3	220	190	265	75	20.9	0.5	9.6
Elec. Cond. (μ cm ⁻¹)	40	407.6	405	376	473	97	21.1	1.4	5.2
Gharabolagh									
Discharge (L s ⁻¹)	42	609.8	590	541	735	194	48.5	0.9	8.0
Elec. Cond. (μ cm ⁻¹)	42	550.1	551.5	523	591	68	15.9	0.3	2.9
Rijab									
Discharge (L s ⁻¹)	42	2275.0	1670	1096	6560	5464	1597.5	1.8	70.2
Elec. Cond. (μ cm ⁻¹)	42	366.3	367	345	385	40	11.8	-0.3	3.2
Sheshpeer									
Discharge (L s ⁻¹)	201	4004.3	3744.2	1493.3	7191.5	5698.2	1351.4	0.5	33.7
Elec. Cond. (μ cm ⁻¹)	18	273.3	275	249	298	49	15.6	0.2	5.7
Berghan									
Discharge (L s ⁻¹)	20	796.3	762.5	345	1348	1003	323.7	0.2	40.6
Elec. Cond. (μ cm ⁻¹)	20	258.7	258.5	252	265	13	3.5	0.2	1.4
Morikosh									
Discharge (L s ⁻¹)	20	106.0	90.5	21	231	210	64.1	0.5	60.5
Elec. Cond. (μ cm ⁻¹)	20	317.0	316.5	308	326	18	4.7	0.3	1.5
Tangkelagari									
Discharge (L s ⁻¹)	21	119.0	82	22	311	289	88.8	0.8	74.6
Elec. Cond. (μ cm ⁻¹)	21	287.6	287	283	295	12	3.1	1.0	1.1
Atashgah									
Discharge (L s ⁻¹)	67	998.7	926.61	733	1533	800	194.7	1.1	19.5
Elec. Cond. (μ cm ⁻¹)	67	283.0	285	263	303	40	7.1	-0.3	2.5
Shosh									
Discharge (L s ⁻¹)	61	82.6	87	40	169	129	30.4	0.7	36.8
Elec. Cond. (μ cm ⁻¹)	61	305.5	304	282	329	47	11.2	0.5	3.7
Enakak									
Discharge (L s ⁻¹)	35	303.4	297	275	341	66	18.6	0.4	6.1
Elec. Cond. (μ cm ⁻¹)	35	351.3	357	221	515	294	77.8	0.1	22.2
Ghomp									
Discharge (L s ⁻¹)	218	887.3	771	527	3031	2504	418.9	3.4	47.2
Elec. Cond. (μ cm ⁻¹)	218	548.2	553	458	707	249	39.1	0.2	7.1

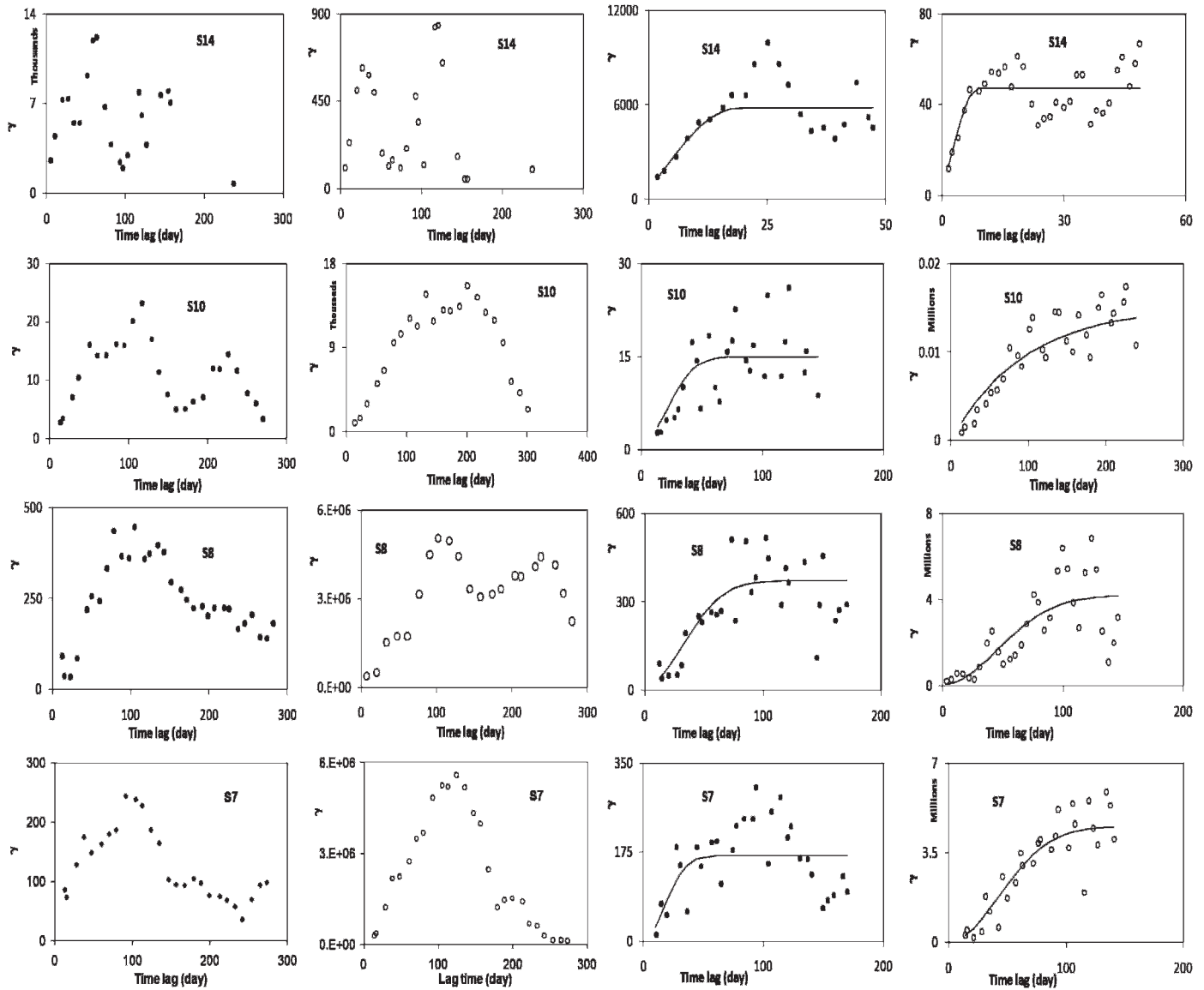


Figure 3. Variograms before (panel 1 and 2 from left) and after removing periodic behavior (panel 3 and 4 from left); solid circles = EC; open circles = discharge.

assumed using the Root Mean Square Error (RMSE), Akaike Information Criteria (AIC) and weighted Sum of Square Error (SSE).

RESULTS

The scatterplots of discharge versus EC and their distributions are shown in Figure 2. Most of the histograms were positively skewed, indicating the presence of large data values for both discharge and EC occurred with low frequency. All histograms were fitted to a lognormal distribution. The descriptive statistics of discharge and EC values for the springs are shown in Table 4.

The correlation among the discharge and EC variables for each spring is shown in Figure 2. Discharge and EC values are positively correlated in Gilan (S1), Sarabgarm (S3), Morikosh (S10), Tangkelagari (S11), and Enakak (S14) Springs, but only partly in Golin (S2), Piran (S5), and Gharabolagh (S6) Springs (Fig. 2). Negative correlation between discharge and EC values is evident for Marab (S4), Rijab (S7), Berghan (S9), Atashgah (S12), Shosh (S13), Ghomp (S15) Springs, but less so in Sheshpir Spring (S8). The strong negative correlation between discharge and EC may be interpreted as an indication of a freshwater recharge signal during the rainy season, which yields a considerable volume of low-EC water. The somewhat constant EC versus discharge values for Piran (S5) and

Table 5. The value of fitting criteria in modeling of periodic variograms after removing the periodicity (the best models are presented by bold numbers).

Spring	Fitting Criteria	Model		
		Exp.	Gau.	Sph.
Sarabgarm				
Discharge	RMSE	23.8	25	22.7
	AIC	287	190	285
	SSE	17	10	11
Elec. Cond.	RMSE	703	727	723
	AIC	484	486	485
	SSE	703	727	723
Marab				
Discharge	RMSE	139,988	138,152	139,014
	AIC	791	790	790
	SSE	391	352	446
Elec. Cond.	RMSE	127	128	127
	AIC	384	385	384
	SSE	20	21	20
Rijab				
Discharge	RMSE	930,689	784,578	854,776
	AIC	869	859	864
	SSE	172	31	102
Elec. Cond.	RMSE	64	61	61
	AIC	345	342	342
	SSE	125	86	124
Sheshpeer				
Discharge	RMSE	1,411,274	1,267,446	1,345,383
	AIC	990	983	987
	SSE	760	246	362
Elec. Cond.	RMSE	102	92	93
	AIC	359	353	353
	SSE	113	83	85
Morikosh				
Discharge	RMSE	1252	1033	1167
	AIC	517	506	513
	SSE	219	35	152
Elec. Cond.	RMSE	11	10	10.8
	AIC	190	186	187
	SSE	25	20	21.6
Tangelagari				
Discharge	RMSE	2083	2011	2008
	AIC	247	545	544
	SSE	38	11	19.4
Elec. Cond.	RMSE	4.7	4.6	4.6
	AIC	172	170	170
	SSE	31	29	36
Shosh				
Discharge	RMSE	267	250	251
	AIC	459	455	455
	SSE	53	43	55

Table 5. Continued.

Spring	Fitting Criteria	Model		
		Exp.	Gau.	Sph.
Elec. Cond.	RMSE	9.6	9.6	9.2
	AIC	252	253	250
	SSE	41	40	32
Enakak Discharge	RMSE	106	79	9.2
	AIC	266	253	250
	SSE	50	26	32
Elec. Cond.	RMSE	1644	1550	1548
	AIC	381	378	378
	SSE	41	37	37
Ghomp Discharge	RMSE	640	377	569
	AIC	427	399	423
	SSE	38	13	33
Elec. Cond.	RMSE	87	91	79
	AIC	389	392	384
	SSE	16	26	16.8

Sheshpir (S8) Springs could be caused by (1) a large underground lake that supplies most of the spring discharge water, but also has the capability of damping EC values, or (2) a small or non-rapid recharge component. Alternatively, the generally positive correlation between discharge and EC values may suggest a piston-flow regime in a less developed karst aquifer, which forces water from temporary detention out into a solution conduit for transit to spring outlets during high-flow periods as a result of rising head in the aquifer. In addition, higher mineralized water may be stored in the epikarst, which may contain soluble formations.

VARIOGRAM TEMPORAL STRUCTURES

The experimental variograms were computed for discharge- and EC-time series data for all springs. Temporal behaviors of springs in terms of variograms is different for discharge- and EC-time series. Two temporal structures are evident in variograms: (1) a periodic behavior and (2) a nugget effect with one or two scales of temporal structures.

Periodicity

Several variograms seem to fluctuate periodically so it is necessary to describe them with a periodic function. One usually observes a variety of temporal periodicities, such as periodic seasonal or annual cycles. The simplest such function is a sine wave (Webster and Oliver, 2001)

$$\begin{aligned}\gamma(h) &= C_1 \cos\theta + C_2 \sin\theta \\ C_1 &= W \cos\phi \\ C_2 &= W \sin\phi \\ \theta &= \frac{2\pi h}{\omega}\end{aligned}\quad (2)$$

where W , ω and ϕ are the amplitude, length of wave, and phase shift, respectively. The variograms of the discharge and EC values indicate two cyclical trends (Fig. 3). The relative impacts of these cycles may vary from spring to spring, as well as from discharge to EC values. For example, Figure 3 clearly illustrates that the Rijab (S7), Morikosh (S10), and Tangkelagari (S11) Springs have much stronger seasonal components (i.e., effects) than do the Sarabgarm (S3), Sheshpir (S8) and Ghomp (S15) Springs. Discharge variograms display a periodic structure in the Sarabgarm (S3), Rijab (S7), Morikosh (S10), Tangkelagari (S11), and Shosh (S13) Springs while the Marab (S4), Rijab (S7), Sheshpir (S8), Morikosh(S10), and Tangkelagai (S11) Springs reflect periodic processes in EC variograms. Variograms for discharge and EC depict periodicity wavelengths for the springs that range from less than 100 days for Enakak Spring (S14) to more than 316 days for Sarabgarm Spring (S3) and from 82 days in Enakak Spring (S14) to more than 300 days in Sheshpir Spring (S8). These differences may be a result of the catchment areas of the springs. Smaller variogram wavelengths were observed for springs characterized by smaller size of catchment area

because of the small distance between the outlet and the hindmost point in the catchment area.

To remove the periodicity and explore the short temporal structures, we use a partial series of discharge and EC values for the springs. These partial series include measured discharge and EC values during a single cyclical period, only. The variograms of these partial time series are shown in Figure 3, and the performance of the different simulation models for temporal behavior of the variograms are presented in Table 5. The variogram parameters (i.e., nugget effect, range(s), and sill(s)) are listed in Table 6 based on the selected best models. The range (A_1 in Table 6) varies from 10 days for Shosh Spring (S13) to 114 days for Marab Spring (S4) and from 9 days for Enakak Spring (S14) to 107 days for Sarabgarm Spring (S3), according to variograms of discharge and EC values, respectively. The range depicts a time length (i.e., discharge and/or EC) with minimum correlation. Therefore, it seems that the contribution of a flow component (e.g., conduit(s) or matrix porosity) gradually increases during the range time scale (A_1) and its effect disappears in spring water.

Nugget Effect and Temporal Structures

Several of the variograms have a small nugget effect and show one or two scales of temporal structures (Fig. 4). The performance of permissible models are evaluated based on performance indexes (Table 7). The best model for simulating temporal behaviors of experimental variograms are then selected (Table 6). The nugget effect is well pronounced for Golin Spring (S2), Piran Spring (S5), and Gharabolagh (S6) Spring (Fig. 4), and this behavior may be caused by (1) measurement error and/or (2) micro-variability (e.g., variability at a scale smaller than the sampling resolution (Kitanidis, 1997)).

Two ranges with different time scales were obtained during the modeling procedure. One and two temporal structures are observed for Gilan Spring (S1), Golin Spring (S2), Berghan Spring (S9), and Tangkelagari Spring (S11), and for Atashgah Spring (S12) and Sheshpir Spring (S8), respectively (Fig. 4). The different temporal behaviors (i.e., the shape of variograms) are likely caused by different karst systems or subsystems within the aquifers.

Short range variations (A_1) occur from 17 days at Berghan Spring (S9) to 268 days at Atashgah Spring (S12) and from 28 days at Berghan Spring (S9) to 110 days at Atashgah Spring (S12) for variograms of discharge and EC, respectively. Range A_1 could be evaluated as an indicator of the length of time that spring water is dominantly supplied by a part of the karst system that contains well-developed solution conduits. The short range length of time is proposed as a measure of residence time for water stored in large solution conduits as being more important for water movement than for water storage. Long range time values (A_2) are estimated to exceed 220 days (Table 6). It would seem that the entire karst system is

responsive to A_2 . Range A_2 may be regarded as a measure of water residence time in the fissured matrix. Temporal values of discharge and EC are uncorrelated after the A_2 time period, suggesting that the contribution of the entire karst system diminishes after this time period. The results of previous studies on residence time of some springs (Karimi, 2003) confirm our findings.

DISCUSSION

Variations in discharge and EC in the studied springs is complex and exhibit varying temporal behaviors. The exploratory data analysis presents the information in a compact format as the first step for determining temporal structure. Plots of the obtained range (A_1) according to variogram analysis versus catchment areas, percent of discharge quick flow (% Q), and ratio of maximum discharge to minimum discharge (Q_{\max}/Q_{\min}) are presented in Figure 5. From Figure 5, it is apparent that springs with small catchment areas have shorter ranges (i.e., residence time) than those springs with larger catchment areas. The higher values of range (A_1) are observed in springs that are characterized by lower percentages of quick flow, as well as the ratio of maximum discharge to minimum discharge (Q_{\max}/Q_{\min}) (Fig. 5).

The discharge and EC variograms provide different ranges (i.e., residence time) for each spring. Differences between the ranges might be a result of influence of the behavior of the karst system that supplies spring water. Differences between the two ranges obtained, based on variograms of discharge and EC for the springs, vary from seven days in Piran Spring (S5) to 158 days in Atashgah Spring (S12) (Table 8). The springs could be classified into three groups based on the percent of difference between the ranges (Table 8): Group 1 springs are those springs with less than 40% differences; Group 2 are those springs with 40 to 70% differences; and Group 3 are those springs with greater than 70% differences. Group 1 includes Golin (S2), Piran (S5), Gharabolagh (S6), Sheshpir (S8) and Berghan (S9) Springs that are characterized by (1) no obvious trend in scatterplots of discharge versus EC values (Fig. 2); and (2) same temporal behavior of variograms of discharge and EC values (Figs. 3 and 4). It would seem that for these springs, spring water may be supported by a large underground karst reservoir. Heavy precipitation events could be damped by this underground reservoir. Accordingly, the temporal behavior of discharge and EC are controlled by the underground reservoir because large precipitation events do not translate into significant discharge increases and EC fluctuations (i.e., sharp increase followed by a significant decrease below the static condition). Small differences between the ranges suggest the possibility of large karst openings that supply spring water. The existence of an underground karst reservoir (or huge solution conduits) supplying water to Sheshpir Spring (S8) was reported by Raeisi and Karami (1997).

Table 6. Parameters of selected variograms.

Spring	Model	C_0^a	C_1^b	A_1^c	C_2^b	A_2^c
Gilan						
Discharge	Gau.	2138	14381	108		
Elec. Cond.	Gau.	172	1414	70		
Golin						
Discharge	Gau.	343	432	98		
Elec. Cond.	Gau.	103	92	126		
Sarabgarm						
Discharge	Sph.	29	75	107		
Elec. Cond.	Exp.	954	2114	69		
Marab						
Discharge	Gau.	28053	254974	46		
Elec. Cond.	Sph.	58	482	114		
Piran						
Discharge	2 Exp.	134	133	88	545	224
Elec. Cond.	Gau.	208	398	95		
Gharabolagh						
Discharge	Sph.	146	122	51		
Elec. Cond.	Gau.	383	3058	41		
Rijab						
Discharge	Gau.	50000	4458351	61		
Elec. Cond.	Gau.	0	167	95		
Sheshpeer						
Discharge	Gau.	82207	4103478	65		
Elec. Cond.	Gau.	16.5	355	47		
Berghan						
Discharge	2 Exp.	0	48541	28	303380	272
Elec. Cond.	2 Sph.	0	0.3	17	27	269
Morikosh						
Discharge	Exp.	0	15041	94		
Elec. Cond.	Gau.	1.2	14	31		
Tangelagari						
Discharge	Gau.	56	6021	60		
Elec. Cond.	Gau.	1.5	24	33		
Atashgah						
Discharge	Sph.	2209	50000	110		
Elec. Cond.	Sph.	1.7	19.5	268		
Shosh						
Discharge	Gau.	420	874	39		
Elec. Cond.	Sph.	0	47	10		
Enakak						
Discharge	Sph.	0	47	9		
Elec. Cond.	Sph.	480	5353	19		
Ghomp						
Discharge	Gau.	484	6636	26		
Elec. Cond.	Sph.	193	750	54		

^a Nugget effect.^b Sill.^c Range.

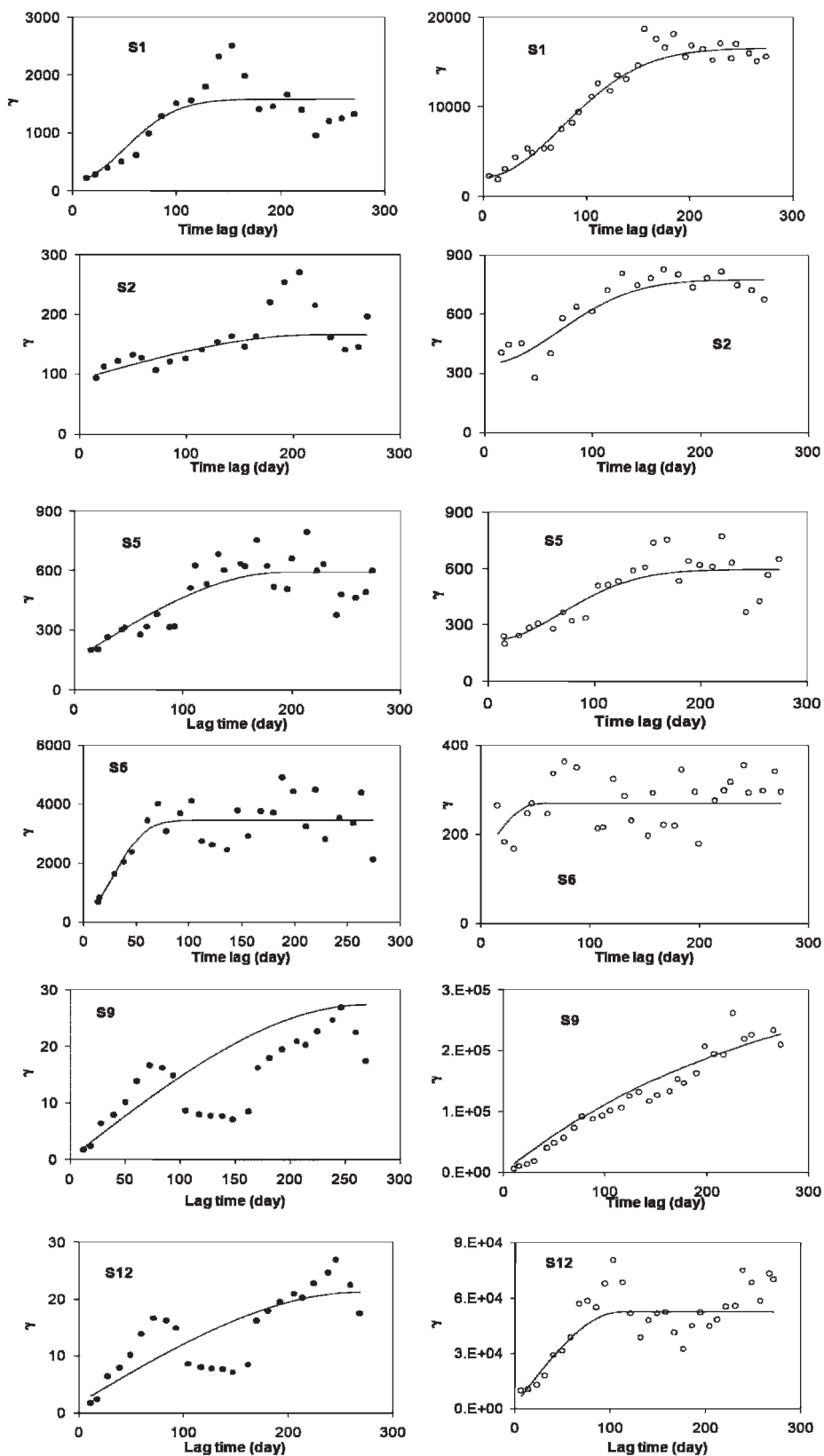


Figure 4. Non-periodic variograms of discharge (right panel) and EC (left panel) values.

Table 7. The value of fitting criteria in modeling of non-periodic variograms (the best models are presented by bold numbers).

Spring	Fitting Criteria	Model				
		Exp.	Gau.	Sph.	Dub. Sph.	Dub. Exp.
Gilan						
Discharge	RMSE	1742	1177	1330	1255	1761
	AIC	575	551	558	558	580
	SSE	9.8	5	6.3	6.9	12.7
Elec. Cond.	RMSE	422	357	373	696	510
	AIC	324	317	319	349	336
	SSE	79	35	34	34	69.5
Golin						
Discharge	RMSE	85	68	71	128	94
	AIC	243	234	236	264	252
	SSE	9.5	6.8	8	20	10
Elec. Cond.	RMSE	38.7	32.7	37.1	34.4	39.3
	AIC	223	216	222	222	228
	SSE	5.1	7.1	4.7	6.8	13.4
Piran						
Discharge	RMSE	99.4	90.4	91	145	112
	AIC	330	325	325	353	395
	SSE	16	13	14	53	21
Elec. Cond.	RMSE	103	93.6	94	96	124.3
	AIC	386	380	381	386	345
	SSE	25.4	20	18.5	19.5	7.3
Gharabolagh						
Discharge	RMSE	59	62	59	96	81
	AIC	353	356	353	386	376
	SSE	17	18	17	40	30
Elec. Cond.	RMSE	684	659	661	1023	851
	AIC	430	428	428	455	445
	SSE	11	9.2	9.3	27	16
Berghan						
Discharge	RMSE	58,067	73,290	60,766	69,655	24,986
	AIC	766	780	769	781	719
	SSE	741	7613	856	503	182
Elec. Cond.	RMSE	4.9	4.8	4.5	4.4	6.5
	AIC	166	165	162	164	184
	SSE	70	75	67	64	125
Atashgah						
Discharge	RMSE	13,574	11,244	11,733	20,497	13,894
	AIC	820.2	806.6	693.4	732	707.9
	SSE	181.1	97.8	116.2	318	194
Elec. Cond.	RMSE	13.8	16.57	4.6	25.4	14
	AIC	275.5	286.5	163.1	262.9	281.8
	SSE	42.5	46.3	70.65	145.4	47.9

Concentrated rapid recharge through the sinkholes is the dominant recharge mechanism for Sheshpir Spring (S8).

Group 2 includes Sarabgarm (S3), Rijab (S7), Tangkelagari (S11) and Enakak (S14) Springs that are character-

ized by (1) a positive correlation between discharge and EC values (Fig. 2); and (2) periodic structures in the variograms but with different temporal behaviors between discharge and EC (Fig. 3). This group may belong to

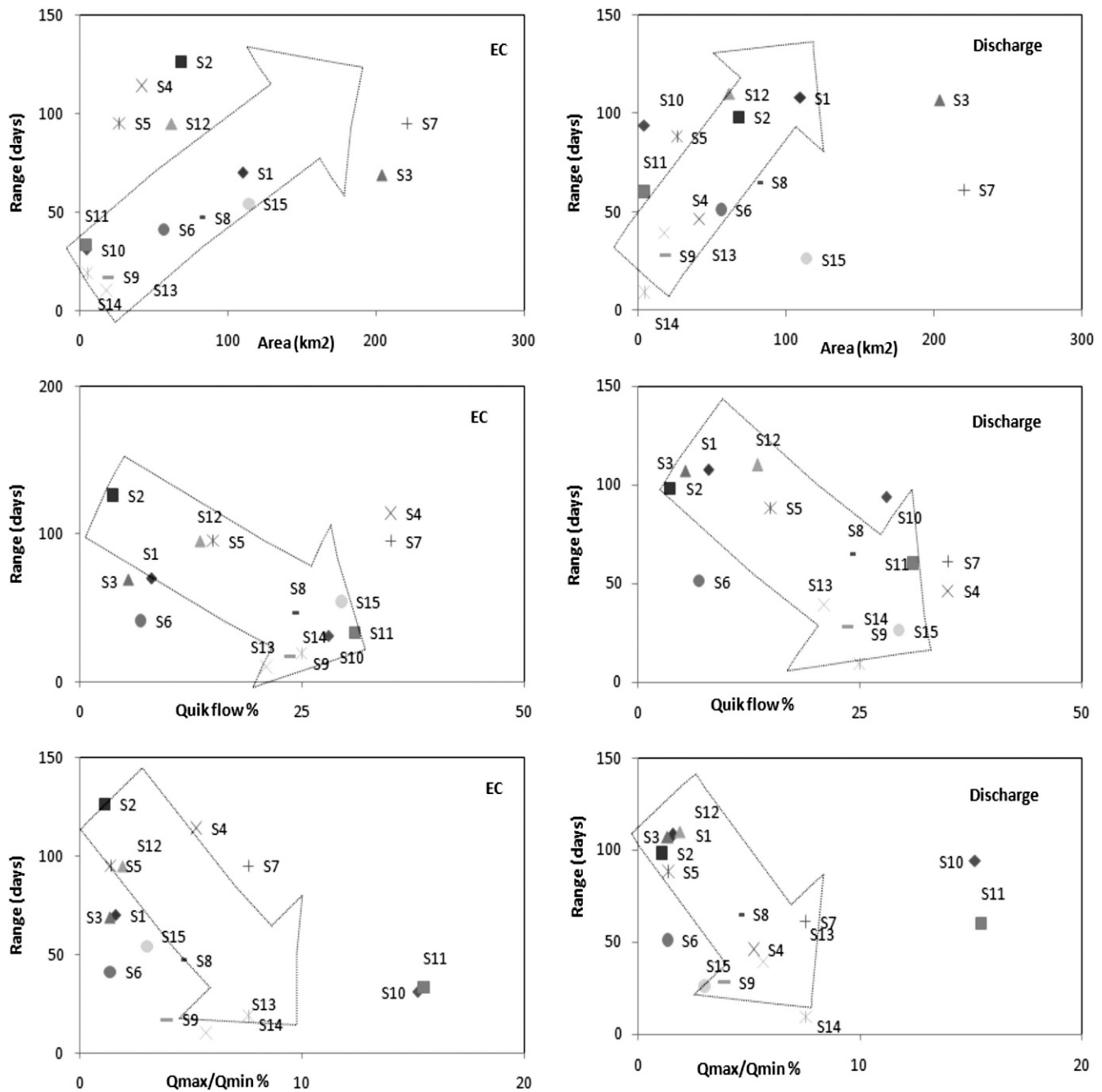


Figure 5. Relationship between residence-time range (A1) and selected characteristics of the springs.

a karst system or subsystem that is poorly developed and is dominantly displaced by a piston-flow regime. Previous findings about Enakak Spring (S14) (Keshavarz, 2003) confirm our interpretation of a karst system or subsystem dominated by a piston-flow regime for Group 2.

Group 3 includes Gilan Spring (S1), Marab Spring (S4), Morikosh Spring (S10), Atashgah Spring (S12), Shosh Spring (S13) and Ghomp Spring (S15), which are subjected

to (1) a negative correlation between discharge and EC values (Fig. 2); and (2) different temporal structure in variograms of discharge and EC (Figs. 3 and 4). We believe this group is supported by a well-developed karst system or subsystem that provides higher discharge values that coincide with lower values of EC. Quick response of the karst system or subsystem to precipitation events causes different temporal behaviors in variograms of discharge and EC.

Table 8. The ratio of difference between obtained ranges based of variograms of discharge (R_Q) and electrical conductivity (R_{EC}).

Spring	Residence Time (d)		$ R_{EC} - R_Q $	$\left\{ \frac{ R_{EC} - R_Q }{\left[\frac{(R_{EC} + R_Q)}{2} \right]} \right\} \times 100$	Group
	Elec. Cond. (R_{EC})	Discharge (R_Q)			
Gilan	70	108	38	43	3
Golin	126	98	28	25	1
Sarabgarm	69	107	38	43	2
Marab	114	46	68	85	3
Piran	95	88	7	8	1
Gharabolagh	41	51	10	22	1
Rijab	95	61	34	44	2
Sheshpir	47	65	18	32	1
Berghan	17	28	9	49	1
Morikosh	31	94	63	100	3
Tangkelagari	33	60	27	58	2
Atashgah	268	110	158	84	3
Shosh	10	39	29	118	3
Enakak	19	9	10	71	2
Ghomp	54	26	28	70	3

Note: EC is electrical conductivity.
 Q is discharge.

CONCLUSIONS

The time series that describe discharge and EC variations at the springs represent aquifer behavior over the time domain. The application of variogram analysis suggests two temporal behaviors characterize the time series of discharge and EC at springs. These temporal behaviors include periodicity and nugget effect plus one or two temporal structures. For the springs studied here, the periodicity ranges from 100 to 316 days and from 82 to 300 days for variogram of discharge and EC, respectively. The temporal structure in one cyclical period is explored by application of variogram on partial data in a cycle.

Some of the variograms are modeled by double exponential or spherical models which introduce two temporal ranges (i.e., A1 and A2). The short range (A1) can be considered as an indication of water residence time in well-developed karst conduits, while the entire karst system is responsive to the long range (A2). The springs are classified into three groups according to differences between ranges obtained by variograms of discharge and EC that belong to the development of karst in each system. The results obtained in this study confirm previous findings of the study area and provide valuable new findings regarding the temporal structure of the aquifers and additional insights into the karst systems. This research also illustrates how variogram analysis can improve our understanding of karst systems by using time series of physico-chemical parameters. The authors propose the

application of variogram analysis on time series of physico-chemical parameters as a part of karst spring studies.

ACKNOWLEDGEMENTS

The authors would like to thank Dr. Arthur N. Palmer of the Earth Science Department of the State University of New York and Dr. Thomas Johnson of the National Center for Environmental Assessment of the U.S. Environmental Protection Agency for their review and constructive criticisms of the manuscript. The authors thank Professor E. Raeisi of the Earth Science Department of the Shiraz University of Iran for providing all data. The first author would like to thank the Research Council of Shiraz University for financial support.

REFERENCES

- Alavi, M., 2004, Regional stratigraphy of the Zagros fold-thrust belt of Iran and its proforeland evaluation: *American Journal of Science*, v. 304, p. 1–20.
- Alavi, M., 2007, Structures of the Zagros fold thrust belt in Iran: *American Journal of Science*, v. 307, p. 1064–1095.
- Bacchi, B., and Kottegoda, N.T., 1995, Identification and calibration of spatial correlation patterns of rainfall: *Journal of Hydrology*, v. 165, p. 311–348.
- Bakalowicz, M., 2005, Karst groundwater: A challenge for new resources: *Hydrogeology Journal*, v. 13, p. 148–160.
- Berne, A., Delrieu, G., Creutin, J.D., and Obled, C., 2004, Temporal and spatial resolution of precipitation fall measurements required for urban hydrology: *Journal of Hydrology*, v. 299, p. 166–179.
- Buytaert, W., Celleri, R., Willems, P., Bievre, B.D., and Wyseure, G., 2006, Spatial and temporal precipitationfall variability in mountain-

- ous areas: A case study from the south Ecuadorian Andes: *Journal of Hydrology*, v. 329, p. 413–421.
- Chambers, J.M., Cleveland, W.S., Kleiner, B., and Tukey, P.A., 1983, *Graphical methods for data analysis*: Murray Hill, N.J., Bell Telephone Laboratories Inc., 395 p.
- Desmarais, K., and Rojstaczer, S., 2002, Inferring source waters from measurements of carbonate spring response to storms: *Journal of Hydrology*, v. 260, p. 118–134.
- Deutsch, C.V., and Journel, A.G., 1992, *GSLIB: Geostatistical software library and user's guide*: New York, Oxford University Press, 340 p.
- Farnham, I.M., Stetzenbach, K.J., Singh, A.K., and Johannesson, K.H., 2000, Deciphering groundwater flow system in Oasis Valley, Nevada, using tracer element chemistry, multivariate statistics and geographical information systems: *Mathematical Geology*, v. 32, no. 8, p. 943–968.
- Ford, D.C., and Williams, P.W., 2007, *Karst hydrogeology and geomorphology*, Chichester: West Sussex, UK, John Wiley & Sons, Ltd, 562 p.
- Gillieson, D., 1996, *Caves: Processes, development, and management*: Cambridge, Mass., Blackwell Publishers, Inc., 324 p.
- Goovaerts, P., 1997, *Geostatistics for natural resources evaluation*: New York, Oxford University Press, 483 p.
- Goovaerts, P., Sonnet, P., and Navarre, A., 1993, Factorial kriging analysis of springwater contents in the Dyle River basin, Belgium: *Water Resources Research*, v. 29, no. 7, p. 2115–2125.
- Hess, J.W., and White, W.B., 1988, Storm response of the karstic carbonate aquifer of south central Kentucky: *Journal of Hydrology*, v. 99, no. 3–4, p. 235–252.
- Holawe, F., and Dutter, R., 1999, Geostatistical study of precipitation series in Austria: Time and space: *Journal of Hydrology*, v. 219, p. 70–82.
- Isaaks, E.H., and Srivastava, R.M., 1989, *An introduction to applied geostatistics*: New York, Oxford University Press, 561 p.
- James, G.A., and Wynd, J.G., 1965, Stratigraphic nomenclature of Iranian Oil Consortium Agreement area: *Bulletin of American Association of Petroleum Geologists*, v. 49, no. 12, p. 2182–2245.
- Karimi, H., 2003, Hydrogeological behaviour of the Alvand basin karst aquifers, Kermanshah [Ph.D. dissertation]: Shiraz, Iran, Shiraz University, 212 p.
- Karimi, H., Raeisi, E., and Zare, M., 2005a, Physicochemical time series of karst springs as a tool to differentiate the source of spring water: *Carbonate and Evaporates*, v. 20, no. 2, p. 138–147.
- Karimi, H., Raeisi, E., and Bakalowicz, M., 2005b, Characterizing the main karst aquifers of the Alvand basin, northwest of Zagros, Iran, by a hydrogeochemical approach: *Hydrogeology Journal*, v. 13, p. 787–799.
- Keshavarz, T., 2003, Study on the karstic artesian aquifers in the Khersan3 Dam site [M.Sc. Thesis]: Shiraz, Iran, Shiraz University, 212 p.
- Kitanidis, P.K., 1997, *Introduction to geostatistics: Application to hydrogeology*: Cambridge University Press, UK, 249 p.
- Kolovos, A., Christakos, G., Hristopoulos, D.T., and Serre, M.L., 2004, Methods for generating non-separable spatiotemporal covariance models with potential environmental applications: *Advances in Water Resources*, v. 27, p. 815–830.
- Kovacs, A., Perrochet, P., Kiraly, L., and Jeannin, P.Y., 2005, A quantitative method for the characterisation of karst aquifers based on spring hydrograph analysis: *Journal of Hydrology*, v. 303, p. 152–164.
- KWPA, 2009, Khuzestan Water and Power Authority, <http://www.kwpa.ir/> [accessed June 22, 2009].
- Kyriakidis, P.C., Miller, N.L., and Kim, J., 2004, A spatial time series framework for simulating daily precipitation at regional scales: *Journal of Hydrology*, v. 297, p. 236–255.
- Larocque, M., Mangin, A., Razack, M., and Banton, O., 1998, Contribution of correlation and spectral analysis to the regional study of a large karst aquifer (Charente, France): *Journal of Hydrology*, v. 205, p. 217–231.
- Lopez-Chicano, M., Bouamama, M., Vallejos, A., and Pulido-Bosch, A., 2001, Factors which determine the hydrogeochemical behavior of karstic springs: A case study from the Betic Cordilleras, Spain: *Applied Geochemistry*, v. 16, p. 1179–1192.
- Manga, M., 1999, On the timescales characterizing groundwater discharge at springs: *Journal of Hydrology*, v. 219, p. 56–69.
- Mangin, A., 1984, Pour une meilleure connaissance des systems hydrologiques a partir des analyses correlative et spectrale: *Journal of Hydrology*, v. 67, p. 25–43.
- Mangin, A., 1994, *Karst hydrogeology*, in Gilbert, J., Danielopol, D.L., and Stanford, J.A., eds., *Groundwater ecology*: San Diego, Academic Press, p. 43–67.
- Milanović, P.T., 1981, *Karst hydrogeology*, Colorado, Water Resources Publications, 434 p.
- Minasny, B., McBratney, A.B., and Whelan, B.M., 2005, VESPER version 1.62. Australian Centre for Precision Agriculture, McMillan Building A05, The University of Sydney, NSW 2006, (<http://www.usyd.edu.au/su/agric/acpa>).
- Mohammadi, Z., and Raeisi, E., 2007, Hydrogeological uncertainties in delineation of leakage at karst dam sites, the Zagros Region, Iran: *Journal of Cave and Karst Studies*, v. 69, no. 3, p. 305–317.
- Mohammadi, Z., Raeisi, E., and Bakalowicz, M., 2007, Evidence of karst from behavior of the Asmari limestone aquifer at the Khersan3 dam site, Southern Iran: *Hydrological Science Journal*, v. 52, no. 1, p. 206–220.
- Moore, G.K., 1992, Hydrograph analysis in fractured rock terrane: *Ground Water*, v. 30, no. 3, p. 390–395.
- Padilla, A., and Pulido-Bosch, A., 1995, Study of hydrographs of karstic aquifers by means of correlation and cross-spectral analysis: *Journal of Hydrology*, v. 168, p. 73–89.
- Palmer, A.N., 2007, *Cave geology*: Dayton, Ohio, Cave Books, 454 p.
- Panagopoulos, G., and Lambrakis, N., 2006, The contribution of time series analysis to the study of the hydrodynamic characteristics of the karst aquifers of Greece (Trifilia, Almyros Crete): *Journal of Hydrology*, v. 329, p. 368–376.
- Pezeshpoor, P., 1991, Hydrogeological and hydrochemical evaluation of Kuh-e Gar and Barm Firooz Springs, [M.Sc. thesis]: Shiraz, Shiraz University, 282 p.
- Raeisi, E., 2004, *Iran cave and karst*, in Gunn, J., ed., *Encyclopedia of Cave and Karst*: New York, Fitzroy Dearborn, p. 460–461.
- Raeisi, E., and Laumanns, M., 2003, *Cave directory of Iran*: Berlin, Berliner Hohlenkundliche Berichte, 101 p.
- Raeisi, E., and Karami, G., 1997, Hydrochemographs of Berghan karst spring (S9) as indicators of aquifer characteristics: *Journal of Cave and Karst Studies*, v. 59, no. 3, p. 112–118.
- Rouhani, S., and Wackernagel, H., 1990, Multivariate geostatistical approach to space–time data analysis: *Water Resources Research*, v. 26, no. 4, p. 585–591.
- Scanlon, B.R., and Thrailkill, J., 1987, Chemical similarities among physically distinct spring types in a karst terrain: *Journal of Hydrology*, v. 89, p. 259–279.
- Silliman, S.E., Boukari, M., Crane, P., Azonsi, F., and Neal, C.R., 2007, Observation on elemental concentrations of groundwater in central Benin: *Journal of Hydrology*, v. 335, p. 374–388.
- StatSoft, Inc., 2001, *Statistica for Windows*, Release 6, Tulsa, Oklahoma.
- Stocklin, J., and Setudehnia, A., 1977, *Stratigraphic lexicon of Iran*, Report No. 18–1971: Tehran, Iran, Geological Survey of Iran, 376 p.
- Webster, R., and Oliver, M., 2001, *Geostatistics for environmental scientists*, Chichester: West Sussex, UK, John Wiley and Sons, Ltd, 271 p.
- White, W.B., 1988, *Geomorphology and hydrology of karst terrains*: Oxford, Oxford University Press, 464 p.